Geotechnical and Geophysical Site Characterisation 5 – Lehane, Acosta-Martínez & Kelly (Eds)

Effect of soil stiffness on cone penetration response in soft-stiff-soft clays

H. Ma, Y. Hu & M. Zhou
School of Civil, Environmental and Mining Engineering, The University of Western Australia, Perth, WA, Australia

M.S. Hossain
Centre for Offshore Foundation Systems, The University of Western Australia, Perth, WA, Australia

ABSTRACT: This paper describes the results from large deformation FE (LDFE) analysis undertaken to provide insight into the influence of soil stiffness, or rigidity index, on cone penetration resistance in three-layer soft-stiff-soft clays. A range of soil stiffnesses were selected encompassing practical interest. A correction factor is proposed for interpreting the actual undrained shear strength of the interbedded stiff layer. The results can assist foundation design in offshore practice.

1 INTRODUCTION

Depletion of known reserves in the shallow waters of traditional hydrocarbon regions is resulting in exploration in deeper, unexplored and undeveloped environments. These are exhibiting more complex soil conditions at the seabed. In emerging provinces and fields, highly layered soils are prevalent. The Sunda Shelf, offshore Malaysia, Australia's Bass Strait and North-West Shelf, Gulf of Thailand, South China Sea, offshore India and Arabian Gulf are particularly problematic in terms of stratigraphy and soil types (InSafeJIP 2010). The difficulty of obtaining high-quality soil samples from these problematic offshore sites has placed increasing reliance on *in situ* testing results.

Currently, the most commonly adopted *in situ* test in offshore site investigations is cone penetration test (CPT). The standard cone penetrometer is cylindrical in shape with a conical tip that has a base area of 10 cm^2 (diameter D = 35.7 mm) and a 60° tip-apex angle, as shown schematically in Figure 1. Parameters measured during a piezocone test include (a) cone tip resistance, q_c; (b) sleeve friction, f_s; and (c) pore water pressure, u_2. This paper considers only cone tip resistance.

The penetration tests are carried out at a rate of v = 20 mm/s. For clay deposits, the velocity is fast enough to ensure undrained conditions. As such, the cone factor N_{kt} is used to relate the net cone tip resistance q_{net} to the intact undrained shear strength s_u as

$$N_{kt} = \frac{q_{net}}{s_u} = \frac{q_t - \sigma_{v0}}{s_u} \quad (1)$$

where q_t is the total cone tip resistance and σ_{v0} is the total overburden stress at the level of the cone shoulder, d (Fig. 1). For this study, the correction for the effect of unequal pore pressure was not necessary as the cone was simulated as a solid shaft (see Fig. 1; i.e. q_t = measured tip resistance q_c).

For stratified seabed sediments, the undrained shear strength for each layer, in particular for the interbedded stiff layer, deduced using Equation 1 may not represent the actual value as the layer thickness may not be sufficient to mobilize the stable (full) penetration resistance for that layer. A corresponding adjustment is required to interpret the actual shear strength. It is also well established that cone penetration resistance is strongly influenced by soil stiffness or rigidity index, which should be taken into account. These are addressed in this paper.

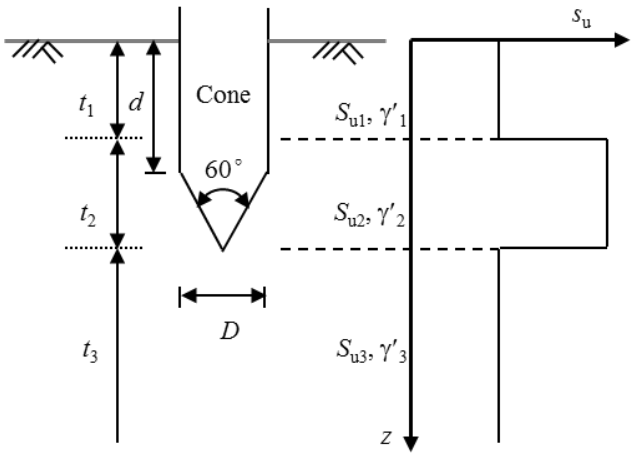

Figure 1. Schematic diagram of cone penetration in soft-stiff-soft clay

For piezocone penetration in single layer clay, the effect of soil rigidity index I_r was quantified through various solutions. These include strain path method (Baligh 1985), hybrid strain path method (Teh & Houlsby 1991), and FE analysis (Yu 2000), large deformation finite element analysis (van den Berg 1994; Lu et al. 2004; Walker & Yu 2006; Liyanapathirana 2009). Recently, Low et al. (2010) assesmbled a worldwide high quality database of lightly overconsolidated clays and used to evaluate the sensitivity of various factors on penetration resistance factors of various penetrometers. It was indicated that I_r has the most significant effect on the cone bearing capacity factor N_{kt}.

Piezocone penetration in layered clays has attracted less attention from researchers. Walker & Yu (2010) carried out analysis for two-layer stiff-soft and three-layer uniform stiff-soft-stiff clays, adopting the linear elastic-perfectly plastic von Mises soil model. The rigidity index of the 1st-2nd-3rd layers were considered as 100-300-100 and 100-500-100, keeping the shear modulus constant (G = 1 MPa) throughout the model. The effects of soil stiffness as well as shear strength have been investigated qualitatively, but no quantitative solutions were given.

Cone penetration in soft-stiff-soft clays has been extensively investigated by Ma et al. (2015) through large deformation finite element (LDFE) analyses. A new design framework was proposed for interpreting the layer boundaries and undrained shear strength of each identified layer. The framework includes a correction factor for interpreting the shear strength of the interbedded stiff layer. The soil rigidity index was considered as constant with I_r =167. In this study, the effect of soil stiffness was particularly explored. The robustness of the correction factor proposed by Ma et al. (2015) was further improved by incorporating the influence of I_r in this paper.

2 NUMERICAL ANALYSES

2.1 *Geometry and parameters*

This study has considered a cylindrical cone penetrometer of diameter D, penetrating into a three-layer deposit as illustrated schematically in Figure 1, where a stiff clay layer with undrained shear strength s_{u2}, effective unit weight γ'_2, and thickness t_2 is sandwiched by two soft layers with identical undrained shear strength $s_{u1} = s_{u3}$ and effective unit weight $\gamma'_1 = \gamma'_3$. The thickness of the top (1st) soft layer is t_1 and that of the bottom (3rd) soft layer is (nominally) infinite. Analyses were undertaken for the standard cone penetrometer of D = 0.0357 m with a 60° tip angle. The soil-cone shaft and soil-cone tip interfaces were modelled as fully smooth (α = 0), using nodal joint elements (Herrmann 1978). From a separate study (Ma et al. 2014), it was found that a smooth cone penetration in non-homogeneous clays resulted insignificant effect of soil strength non-homogeneity on cone penetration resistance. As such, uniform strength was considered for all three layers.

A survey was carried out through offshore geotechnical characterization reports to select realistic soil parameters for parametric study. The three-layer geometries considered here are commonly encountered in the Gulf of Thailand and Sunda Shelf, including Java Sea, as reported by Castleberry and Prebaharan (1985); Handidjaja et al. (2004); Kostelnik et al. (2007); Chan et al. (2008); Osborne et al. (2009). For uniform three-layer clay sediments, the undrained shear strength of stiff clay ranges from 40 to 120 kPa, while that of soft clay varies between 10 and 40 kPa.

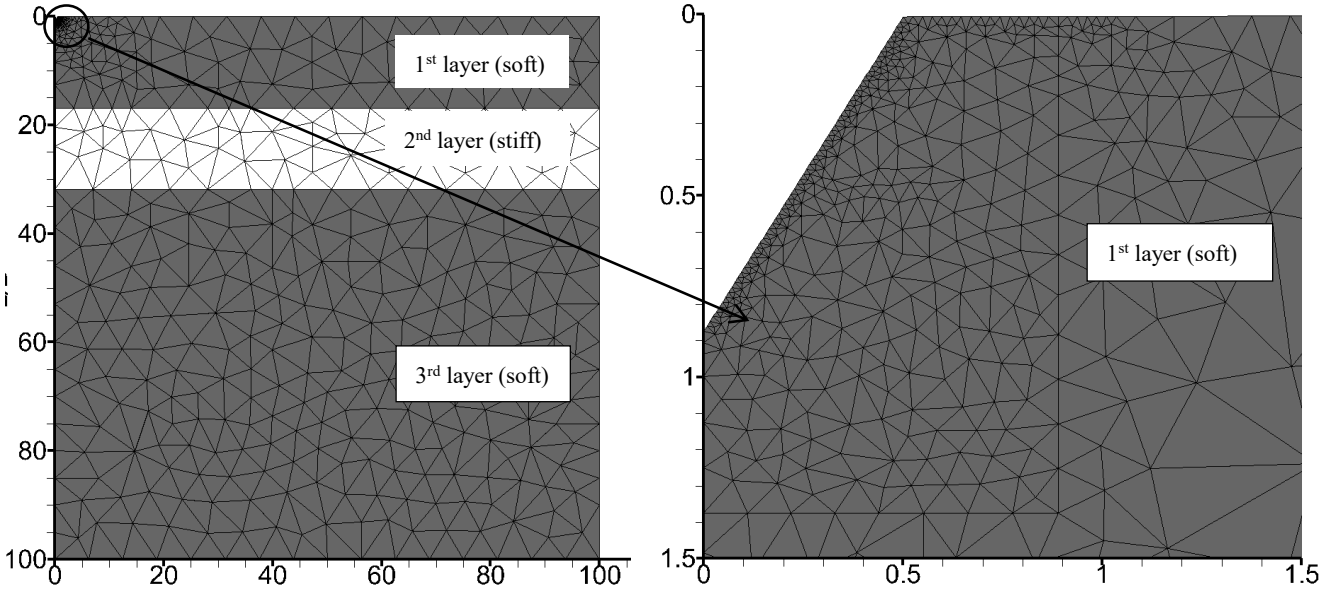

Figure 2. Initial mesh for cone penetration in soft-stiff-soft clay (axes normalized by cone diameter D)

2.2 *Analysis details*

Finite element analyses were performed using the finite element package AFENA (Carter & Balaam 1995) developed at the University of Sydney. *H*-adaptive mesh refinement cycles (Hu & Randolph 1998b) were implemented to optimize the mesh, minimizing discretization errors, concentrating in the most highly stressed zones. Large deformation FE (LDFE) analyses were undertaken using RITSS (Remeshing and Interpolation Technique with Small Strain; Hu & Randolph 1998a). This method falls within what are known as arbitrary Lagrangian-Eulerian (ALE) finite element methods (Ponthot & Belytschko 1998). The details of the LDFE/RITSS approach can be found in Hu & Randolph 1998a. The displacement increment size and the number of steps of small strain analysis between each re-meshing were chosen such that the cumulative penetration between re-meshing stages remained in the small strain range and was less than half the minimum element size.

The axisymmetric soil domain was chosen as 100*D* in radius and 100*D* in depth to ensure that the boundaries were well outside the plastic zone. Hinge and roller conditions were applied along the base and vertical sides of the soil domain respectively. Six-noded triangular elements with three internal Gauss points were used in all the FE analyses. A typical initial mesh for the cone penetration in a three-layer soft-stiff-soft clay deposit is shown in Figure 2, with the cone tip just penetrated into the ground. A fine mesh was considered around the cone tip to ensure the accuracy of the computed results.

The soil was modelled as a linear elastic-perfectly plastic material obeying a Tresca yield criterion. A uniform stiffness ratio of E/s_u = 500 (Zhou et al., 2013) was taken throughout the stratified profiles, except in the exploration of the effect of soil rigidity (I_r), where variation was set up accordingly. Considering the relatively fast penetration of the field cone penetrometer (v = 20 mm/s), all the analyses simulated undrained conditions and adopted a Poisson's ratio $\nu = 0.49$ (sufficiently high to give minimal volumetric strains, while maintaining numerical stability) and friction and dilation angles $\phi = \psi = 0$ in total stress analysis. The geostatic stress conditions were modelled using $K_0 = 1$, as the stable penetration resistance has been found to be unaffected by the value of K_0 (Zhou & Randolph 2009; Low et al. 2010).

3 RESULTS AND DISCUSSION

LDFE analyses were first carried out for three-layer clays with equal strength i.e. $s_{u1} = s_{u2} = s_{u3}$, but varying rigidity index I_r as 50, 150, 300 and 500. Deep bearing capacity factor N_{kt} was calculated according

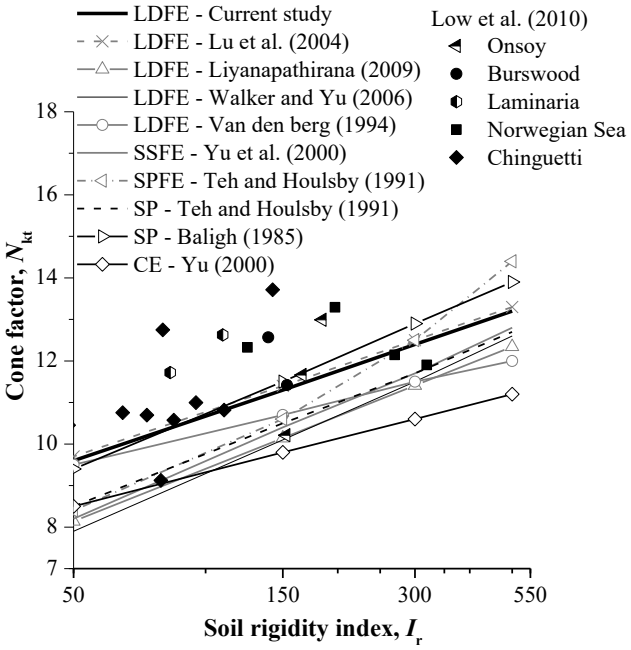

Figure 3. Effect of soil rigidity index on piezocone deep bearing capacity factor N_{kt}

to Equation 1. Figure 3 shows a comparison between the results from this study and existing solutions and laboratory test data of lightly overconsolidated clays in single layer uniform clays (as noted previously). It can be seen that, for the considered smooth cone ($\alpha = 0$), the cone factors derived from the current work agree well with the LDFE results by Lu et al. (2004), lower than the strain path solutions by Baligh (1985) and higher than all other results. The factors lie below the laboratory test data, which may be due to the consideration of fully smooth interface. Generally, bearing capacity factor increases as the soil rigidity index increases, the values from this study can be approximated as

$$N_{kt} = 3.47 + 1.56 I_r \quad (2)$$

For investigation on three-layer deposits, the relative thickness of the top layer t_1/D was deliberately kept constant as 16.8 so that all penetration resistance profiles attain its steady state response in the top layer prior to be influenced by the underlying stiff layer. A typical profile is illustrated in Figure 4 to define the steady state response for each layer and correction factor *k*. As discussed previously, the measured resistance profile in the 2nd (stiff) layer may not reach the steady state prior to dropping its value by sensing the bottom soft layer. This means full resistance of the layer may not be achieved. The strength interpreted using the measured value will then provide a misleading value – lower than the true value.

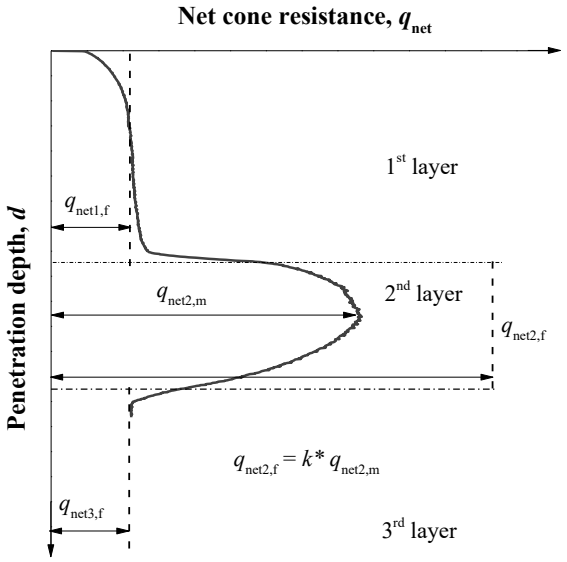

Figure 4. Typical penetration resistance profile in soft-stiff-soft clay and thin-layer correction factor k for 2nd layer

Therefore, following Robertson & Fear's (1995) suggestion, a correction factor k (as described in Fig. 4) is introduced defining as the ratio of the actual full net resistance to measured peak net resistance

$$k = \frac{q_{\text{net2,f}}}{q_{\text{net2,m}}} \tag{3}$$

where $q_{\text{net2,f}}$ and $q_{\text{net2,m}}$ are the actual full and measured peak/maximum net resistance in the 2nd layer respectively. It is found that k is a function of t_2/D, s_{u2}/s_{u3}, and I_{r2}/I_{r3} with the effect of former two dimensionless factors were discussed by Ma et al. (2015).

In order to systematically investigate the effect of soil rigidity index, analyses have been carried out, considering different combinations of soil rigidity indices. Figure 5a plots the values of k for $I_{r3} = I_{r1} = 50$, $I_{r2}/I_{r3} = 1$, 2, 3.34, and 6.68, while the 2nd layer thickness ratio t_2/D ranges from 2 to 20 and strength ratio s_{u2}/s_{u3} varies between 2 and 8. The horizontal axis x_1 is defined as a combined variable of strength ratio s_{u2}/s_{u3} and 2nd layer thickness ratio t_2/D

$$x_1 = \frac{\left(s_{u2} / s_{u3}\right)^{0.5}}{\left(t_2 / D\right)} \tag{4}$$

From Figure 5a, it is seen that the value of correction factor k increases with increasing stiffness ratio I_{r2}/I_{r3} and strength ratio s_{u2}/s_{u3}, and decreases with increasing thickness ratio t_2/D. For each I_{r2}/I_{r3}, the values of k form a linear distribution. When $x_1 = 1$, k equals to 1.53, 1.66, 1.75 and 1.88 for $I_{r2}/I_{r3} = 1$, 2, 3.34, 6.68.

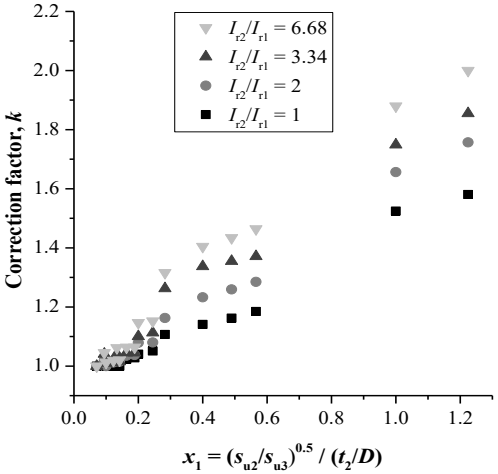

(a) $I_{r1} = I_{r3} = 50$

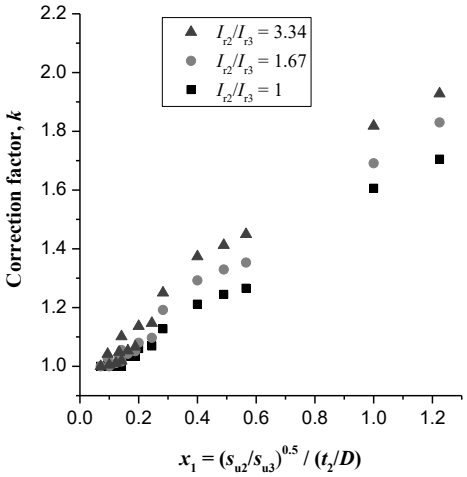

(b) $I_{r1} = I_{r3} = 100$

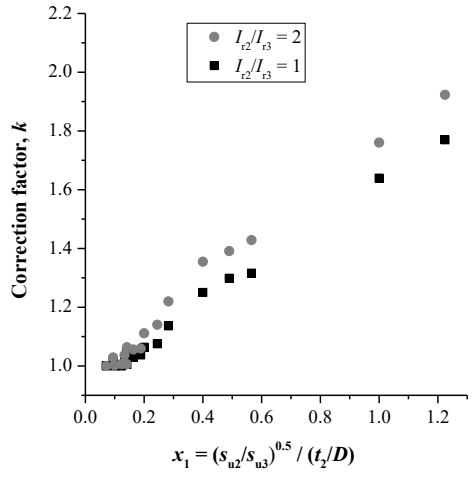

(c) $I_{r1} = I_{r3} = 167$

Figure 5. Values of correction factor k for 2nd layer

Similarly, Figures 5b and c plot the values of k for $I_{r3} = I_{r1} = 100$ and $I_{r2} = 167$. By comparing Figures 5a, b and c, it is seen that the values of k increase with in-

creasing I_{r3}, and the gap gradually reduces with increasing rigidity index ratio I_{r2}/I_{r3}. For instance, for I_{r2}/I_{r3} = 1, 3.34 and x_1 = 1, the lowest correction factor k = 1.53, 1.75 for $I_{r3} = I_{r1}$ = 50, which are respectively about 5.0%, 3.8% lower than those for $I_{r3} = I_{r1}$ = 100 (see Figs 5a and b). The rate of increasing k with I_{r3} also reduces for higher I_{r3}. For instance, for I_{r2}/I_{r3} = 1 and x_1 = 1, k = 1.53, for $I_{r3} = I_{r1}$ = 50, which is increased by 5.2% for $I_{r3} = I_{r1}$ = 100 and 7.5% for $I_{r3} = I_{r1}$ = 167 (see Figs 5a~c). In short, k is a function of I_{r2}/I_{r3} as well as I_{r3}.

To propose a general expression for k taking the influencing factors into account, all values of k plotted in Figure 6 incorporating I_{r2}/I_{r3} and I_{r3} in the horizontal axis. This gives a unique relationship for the correction factor k. A best fit through the data allows k to be approximated as (see Fig. 6)

$$k = \begin{cases} 0.909 + 0.305x_2 - 0.016x_2^2 & \text{for } x_2 \geq 0.35 \\ 1 & \text{for } x_2 < 0.35 \end{cases} \qquad (5)$$

$$x_2 = I_{r3}^{0.2} \times \left(I_{r2}/I_{r3}\right)^{0.3} \frac{\left(s_{u2}/s_{u3}\right)^{0.5}}{\left(t_2/D\right)}$$

As s_{u2} is an input parameter for calculating k, and some iteration is necessary between Equation 3 and 5. An initial value of s_{u2} can be calculated using measured $q_{net2,m}$ and bearing factor N_{kt} (from Equation 2). Then Equations 5, 3 and 2 should be used to calculate k and $q_{net2,f}$ and s_{u2}. Iteration should be continued until the difference between initial and updated s_{u2} becomes less than 3% (Ma et al. 2015).

4 CONCLUDING REMARKS

This paper reports the results from an extensive numerical investigation on soft-stiff-soft clay deposits, simulating continuous penetration of the standard cone penetrometer from the seabed surface. For interpreting the actual undrained shear strength of the interbedded stiff layer, a robust design chart, along with an expression, is proposed incorporating the effects of the interbedded stiff layer strength ratio, thickness ratio and rigidity index ratio.

5 ACKNOWLEDGEMENTS

The research presented here was undertaken with support from the Australian Research Council (ARC) Discovery Grant DP140103997. The fourth author is an ARC Discovery Early Career Researcher Award (DECRA) Fellow and is supported by the ARC Project DE140100903. The work forms part of the activities of the Centre for Offshore Foundation Systems (COFS), currently supported as a node of the Australian Research Council Centre of Excellence for Geotechnical Science and Engineering and as a Centre of Excellence by the Lloyd's Register Foundation. This support is gratefully acknowledged.

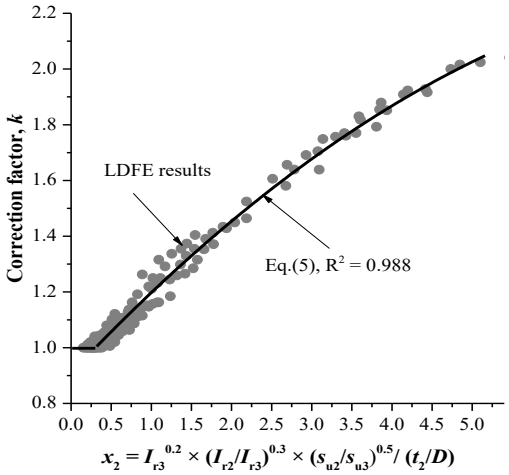

Figure 6. Design chart for correction factor k accounting for effect of soil stiffness

6 REFERENCES

Baligh, M. M. 1985. Strain path method. *Journal of Geotechnical Engineering*, 111(9), 1108-1136.

Carter, J. P. & Balaam, N. P. 1995. *AFENA users' manual*. Centre for Geotechnical Research, Department of Civil Engineering, University of Sydney, Australia.

Castleberry II, J. P. & Prebaharan, N. 1985. Clay crusts of the Sunda Shelf: a hazard to jack-up operations. *Proc. 8th Southeast Asian geotechnical conference*, Kuala Lumpur, 40-48.

Chan, N., Paisley, J. & Holloway, G. 2008. Characterization of soils affected by rig emplacement and Swiss cheese operations-Natuna Sea, Indonesia, a case study. *Proc. 2nd Jack-up Asia Conference and Exhibition*, Singapore.

Handidjaja, P., Somehsa, P. & Manoj, M. 2004. "Swiss-cheese" – A method of degrading soil crust and minimizing risk to punch through problem on the installation of mobile offshore drilling unit (MODU). *Proc. 15th Southeast Asian Geotechnical Society Conference*, Bangkok, Thailand, 303-306.

Herrmann, L. R. 1978. Finite element analysis of contact problems. *Journal of the Engineering Mechanics Division*, 104(5), 1043-1057.

Hu, Y. & Randolph, M. F. 1998a. A practical numerical approach for large deformation problems in soil. *International Journal for Numerical and Analytical Methods in Geomechanics*, 22(5), 327-350.

Hu, Y. & Randolph, M. F. 1998b. H-adaptive FE analysis of elasto-plastic non-homogeneous soil with large deformation. *Computers and Geotechnics*, 23(1-2), 61-83.

InSafeJIP (2010). *Improved guidelines for the prediction of geotechnical performance of spudcan foundations during installation and removal of jack-up units*. RPS Energy, Abingdon, Oxfordshire, UK.

Kostelnik, A., Guerra, M., Alford, J., Vazquez, J. & Zhong, J. (2007). Jackup mobilization in hazardous soils. *SPE Drilling & Completion*, 22(1), 4-15.

Liyanapathirana, D. S. 2009. Arbitrary Lagrangian Eulerian based finite element analysis of cone penetration in soft clay. *Computers and Geotechnics*, 36(5), 851-860.

Low, H. E., Lunne, T., Randolph, M. F., Li, X., Andersen, K. H. & Sjursen, M. A. 2010. Estimation of intact and remoulded undrained shear strengths from penetration tests in soft clays. *Géotechnique*, 60(11), 843-859.

Lu, Q., Randolph, M. F., Hu, Y. & Bugarski, I. 2004. A numerical study of cone penetration in clay. *Géotechnique*, 54(4), 257-267.

Ma, H., Zhou, M., Hu, Y. & Hossain, M. S. 2014. Large deformation FE analyses of cone penetration in single layer non-homogeneous and three-layer soft-stiff-soft clays. *Proc. 33rd Int. conf. on Ocean, Offshore and Arctic Engineering* (OMAE), San Francisco, 23709.

Ma, H., Zhou, M., Hu, Y. & Hossain, M. S. 2015. Interpretation of layer boundaries and shear strengths for soft-stiff-soft clays using CPT data: LDFE analyses. *Journal of Geotecnical and Geoenvironmental Engineering*, DOI: 10.1061/(ASCE)GT.1943-5606.0001370.

Osborne, J. J., Houlsby, G. T., Teh, K. L., Bienen, B., Cassidy, M. J., Randolph, M. F. & Leung, C. F. 2009. Improved guidelines for the prediction of geotechnical performance of spudcan foundations during installation and removal of jack-up units. *Proc. 41st Offshore Technology Conference*, Houston, OTC20291.

Ponthot, J.-P. & Belytschko, T. 1998. Arbitrary Lagrangian-Eulerian formulation for element-free Galerkin method. *Computer methods in applied mechanics and engineering*, 152(1-2), 19-46.

Robertson, P. K. & Fear, C. E. 1995. Liquefaction of sands and its evaluation. *Proc., 1st Int. Conf. on Earthquake Geotechnical Engineering*, Tokyo, 3, K. Ishihara, ed., A. A. Balkema, Rotterdam, the Nederlands, 1253-1289.

Teh, C. I. & Houlsby, G. T. 1991. An analytical study of the cone penetration test in clay. *Géotechnique*, 41(1), 17-34.

van den Berg, P. 1994. *Analysis of soil penetration*. Ph.D. thesis, Delft University, the Netherlands.

Walker, J. & Yu, H. S. 2006. Adaptive finite element analysis of cone penetration in clay. *Acta Geotech.*, 1(1), 43-57.

Walker, J. & Yu, H. S. 2010. Analysis of the cone penetration test in layered clay. *Géotechnique*, 60(12), 939-948.

Yu, H. S. 2000. *Cavity expansion methods in geomechanics*. Kluwer Academic, Dordrecht, the Netherlands.

Zhou, H. & Randolph, M. F. 2009. Numerical investigations into cycling of full-flow penetrometers in soft clay. *Géotechnique*, 59(10), 801-812.

Zhou, M., Hossain, M.S., Hu, Y. & Liu, H. 2013. Behaviour of ball penetrometer in uniform single- and double-layer clays. *Géotechnique*, 63(8), 682-694.